



Green Synthesis, Characterization and *In Vitro* Antioxidant Activity of Silver Nanoparticles from Aqueous Candle Bush (*Senna alata*) Leaf Extract



¹Onojah, Ceasar W., ^{*1}Larayetan, Rotimi A., ²Omatola, Kingsley M., ¹Adegbe, Amanabo M., ¹Abah, Sunday, ¹Abu, Arome, ³Aningo, Gloria N. and ⁴Ogunmola, Oluranti O.

¹Department of Pure and Industrial Chemistry, Kogi State University, Kogi State, Anyigba, Nigerdsia

²Department of Physics, Kogi State University, Kogi State, Anyigba, Nigeria

³Department of Chemistry, Kogi State College of Education (technical), P.O.B, 242, Kabba, Nigeria

⁴Chemistry Unit, Department of Physical Sciences Education, Emmanuel Alayande University of Education, P.M.B 1010, Oyo, Nigeria

*Corresponding Author's email: timlarayetan@gmail.com Phone: +2348030510909

KEYWORDS

Green synthesis,
AgNPs,
Characterization,
TEM,
SEM,
XRD.

ABSTRACT

Green synthesis of AgNPs has become a preferred method over chemical and physical approaches because it is eco-friendly, cost-effective, and avoids the use of toxic chemicals. *Senna alata*, commonly known as Candle Bush, is a medicinal plant widely used in traditional medicine for treating skin infections, diabetes, and inflammatory diseases. This study assesses the phytochemical content and antioxidant activity of *Senna alata* leaf extract, which is used in the environmentally friendly manufacture of silver nanoparticles. Both qualitative and quantitative phytochemical screening revealed a high concentration of bioactive chemicals, with the main ingredients being flavonoids (638.88 ± 4.45 mg/100 g), tannins (665.45 ± 10.29 mg/100 g), and phenols (941.32 ± 10.56 mg/100 g). The biosynthesized AgNPs have been characterized by various analytical techniques such as TGA/DTA, TEM, SEM, and EDS. TEM analysis revealed spherical nanoparticles within the size range of 2.70–6.37 nm. TGA confirmed good thermal stability up to a temperature of 400°C. SEM showed the structures to be of irregular porosity with sizes varying between 100 nm and 9 μ m, whereas EDS showed silver as the major constituent (50.58 wt %). Antioxidant activity was evaluated by DPPH and ABTS assays. The nanoparticles demonstrated higher DPPH radical scavenging activity (IC_{50} : 0.129 mg/mL) than that of the crude extract (IC_{50} : 0.134 mg/mL), while showing similar ABTS radical scavenging activities (IC_{50} : 0.943 and 0.954 mg/mL, respectively). These results indicated that *S. alata*-mediated synthesis of AgNPs is a very promising eco-friendly approach toward developing nanoparticles with improved antioxidant properties that can be useful in pharmaceutical and biomedical applications.

CITATION

Onojah, C. W., Larayetan, R. A., Omatola, K. M., Adegbe, A. M., Abah, S., Abu, A., Aningo, G. N., & Ogunmola, O. O. (2025). Green Synthesis, Characterization and In Vitro Antioxidant Activity of Silver Nanoparticles from Aqueous Candle Bush (*Senna alata*) Leaf Extract. *Journal of Science Research and Reviews*, 2(1), 133-146. <https://doi.org/10.70882/josrar.2025.v2i1.55>

INTRODUCTION

The fields of physics, chemistry, biology, engineering, and nanotechnology are all combined to form nanotechnology. Microorganisms are inhibited and rendered inactive by silver nanoparticles (AgNPs) (Loganathan *et al.*, 2022). Ionic silver and compounds produced from silver are used as antibacterial agents since they are known to be deadly to microorganisms (Kedziora *et al.*, 2021; Wulandari *et al.*, 2022). Microbial cell cultures are not necessary for the production of nanoparticles by plants. Numerous studies have been conducted on the antibacterial properties of silver dressings, silver nitrate, silver zeolite, and AgNPs (Rai *et al.*, 2012). AgNPs derived from biological and plant sources have remarkable qualities in chemical reaction catalysts, optical receptors, non-linear optics, interspersed materials for batteries, bio-labeling, and antibacterial properties (Singh *et al.*, 2023). The creation of plant-mediated nanoparticles is quick and simple. When synthesizing AgNPs, size and form must be taken into account for their physiochemical properties and self-assembly (Herreo *et al.*, 2022). The primary use of silver and AgNPs in medicine is to prevent burn and wound infections, for example, in topical ointments (Boateng, 2020). This plant has expectorant, antibacterial, antifungal, and anticancer qualities in its roots, leaves, and flowers (Osunga *et al.*, 2023). Many skin conditions, such as syphilis sores, ringworm, bronchitis, eczema, ringworm, constipation, asthma, diabetes, diabetic ringworm, snakebite, scorpion bite, itching, mycosis, eczema, ringworm, bronchitis, and urinary tract issues, can also be treated with them (Chua *et al.*, 2019; Fatmawati *et al.*, 2020). For nanotechnology applications, this has speed up research on synthesis paths that improve form and size control. AgNP synthesis using environmentally benign sources, such as plant extract, offers numerous benefits for pharmacological and biological uses (Ahmad *et al.*, 2024).

A member of the Fabaceae subfamily of the Leguminosae, *Senna alata* (also known as *Candle bush*), is used in traditional medicine. According to Osunga *et al.* (2023), this plant's roots, leaves, and petals have expectorant, antibacterial, antifungal, and anticancer qualities. They can also be used to treat a number of skin conditions, such as syphilis sores, ringworm, bronchitis, eczema, constipation, asthma, diabetes, diabetic ringworm, snakebite, scorpion bite, itching, mycosis, eczema, ringworm, bronchitis, and urinary tract issues (Chua *et al.*, 2019; Fatmawati *et al.*, 2020). This research aims to demonstrate the potential of *Senna alata* plant extract as an alternative to hazardous chemicals in the reduction of AgNO₃ to AgNPs and evaluate the antiradical properties of the aqueous leaf extract in relation to the AgNPs made from it. Also the characterization of the biosynthesized nanoparticles using different modern techniques, like UV-

visible spectra, Fourier transformed infrared spectrophotometers (FT-IR), scanning electron microscopes (SEM), Electron diffraction spectrophotometers (EDS), and X-ray diffractometers (XRD).

MATERIALS AND METHODS

Materials and Reagents

The materials and reagents used for the production of the silver nanoparticles are fresh candle bush (*Senna alata*) leaves, silver nitrate (AgNO₃), distilled water, magnetic stirrer or shake, water bath, Whatman No. 1 filter paper, ethanol etc.

Methods

Collection and Preparation of Aqueous Leaf Extract

Fresh candle bush (*Senna alata*) plant parts (leaves) were gathered from the Garden of Emmanuel Alayande College of Education in Oyo town, Nigeria. They were then allowed to air dry for roughly 27 days at room temperature before being pulverized in a Polymix, PX-MFC 90D, mechanical grinder. Approximately 100 g of the crude powdered samples were soaked in 800 mL of distilled water and shaken on an orbital shaker for 24 hours. The solution was filtered through Whatman No. 1 filter paper, and the filtrate was lyophilized into dry powder and was stored carefully in sealed centrifuge tubes under a control temperature of 4 °C until needed for silver nanoparticle synthesis.

Preparation of silver nitrate salt (1 mM)

A 1 mM solution of silver nitrate was prepared by dissolving 0.17 g of AgNO₃ salt having a molar mass of 169.87 g/mol in distilled water. First, the given amount of the salt was weighed by using an analytical balance and was first dissolved in 50 mL of distilled water. The solution was well swirled to obtain complete dissolution and uniform concentration of the salt. It was then transferred to a 1000 mL volumetric flask and then added up to the volumetric flask mark with distilled water.

Qualitative Phytochemical Screening of Candle Bush (*Senna alata*) Leaf Extracts

S. alata leaf extract was subjected to a qualitative phytochemical screening process utilizing established techniques for identifying a drug's phytochemical ingredients (Gunjal, 2022)

Alkaloid Test

To test for alkaloids, 2 drops of Hager's reagent were added to 2 mL of *Senna alata* aqueous extract. The formation of yellow precipitates confirmed the presence of alkaloids.

Phenol Test

A few drops of 5% ferric chloride solution were added to the aqueous extract. The appearance of a dark green or bluish-black color indicated the presence of phenols.

Tannin Test

In this test, 2 mL of *Senna alata* aqueous extract was mixed with an equal volume of water, followed by the addition of 2–3 drops of 5% ferric chloride solution. The development of a blue-black or green color confirmed the presence of tannins.

Flavonoid Test (NaOH Test)

To detect flavonoids, 5 mL of 10% sodium hydroxide solution was added to 5 mL of the aqueous extract. The formation of a yellow-colored solution indicated the presence of flavonoids (Larayetan *et al.*, 2019).

Steroid Test

For this test, 2 mL of *Senna alata* aqueous extract was combined with 2 mL of chloroform, followed by the careful addition of 2 mL of concentrated sulfuric acid. The presence of steroids was confirmed by the appearance of a reddish-brown ring at the junction of the two layers.

Terpenoids Test

To test for terpenoids, 5 mL of *Senna alata* aqueous extract was mixed with 2 mL of chloroform. Then, 3 mL of concentrated sulfuric acid was carefully added to form a separate layer. The development of a deep red color at the interface indicated the presence of terpenoids.

Saponin Test

A diluted extract solution was vigorously shaken for 30 seconds and then left to stand for 30 minutes. The presence of persistent foaming in the test tube confirmed the presence of saponins.

Flavonoid Test (NaOH Test)

As an additional confirmation for flavonoids, 5 mL of 10% sodium hydroxide solution was mixed with 5 mL of the aqueous extract. The resulting yellow solution indicated the presence of flavonoids.

Quantitative Phytochemical Screening

The following quantitative phytochemical screening was conducted on the lyophilized aqueous extract of *Senna alata*:

Determination of Total Phenolic Content

The total phenolic content of *Senna alata* lyophilized extract was determined using the Folin–Ciocalteu reagent method, following the procedure outlined by Waterhouse (2002). In essence, a stock solution of the extract was

prepared at a concentration of 1 mg/mL in methanol. From this stock, 200 μ L of the extract was taken and diluted to a final volume of 3 mL with distilled water. Next, 0.5 mL of Folin–Ciocalteu reagent was added, and the mixture was allowed to react for 3 minutes. After that, 2 mL of a 20% (w/v) sodium carbonate solution was introduced to the reaction mixture. The solution was then left undisturbed in the dark for 60 minutes. Following the incubation period, the absorbance of the sample was measured at 650 nm. The total phenolic content was quantified using a calibration curve constructed with gallic acid, with concentrations ranging from 50 to 500 mg/mL ($r^2 = 0.998$). The results were expressed as milligrams of gallic acid equivalent (GAE) per gram of dry weight.

Determination of Total Tannin Content

Tannin determination was performed by the method of (Gupta *et al.*, 2014) using tannic acid as a standard. In a conical flask, 250 mg of the lyophilized *Senna alata* extract was added to 50 mL of distilled water and shaken in a mechanical shaker for one hour. It was then filtered in a 50-mL volumetric flask and filled the volume with distilled water. Two milliliters (10-fold dilution) of 0.1 M FeCl_3 in 0.1 M HCl were added to an aliquot (1 mL) of the filtrate that had been mixed with four milliliters of distilled water and 0.008 M potassium ferrocyanide. The absorbance at 605 nm of the resulting solution was read after mixing thoroughly and waiting for 10 minutes using the blank as the base of the reading. Quantification was done according to the standard calibration curve of tannic acid in seven points in concentration: 20, 40, 60, 80, 100, 140, and 200 mg/L in distilled water. The results of tannins are given in terms of tannic acid equivalent in milligrams per 100 g of dry material.

Determination of Total Flavonoids Content

The total flavonoid content of the crude extracts was determined using the aluminum chloride colorimetric method, following the procedure described by Chang *et al.* (2002). In summary, a stock solution of the *Senna alata* lyophilized extract was prepared at a concentration of 1 mg/mL. From this, 50 μ L of each extract was taken and diluted to 1 mL using methanol. The solution was then mixed with 4 mL of distilled water, followed by the addition of 0.3 mL of 5% sodium nitrite (NaNO_2) solution. After allowing the mixture to incubate for 5 minutes, 0.3 mL of 10% aluminum chloride (AlCl_3) solution was added and left to stand for another 6 minutes. Subsequently, 2 mL of 1 M sodium hydroxide (NaOH) was introduced, and the final volume was adjusted to 10 mL with double-distilled water. The mixture was allowed to stand for 15 minutes, after which its absorbance was measured at 510 nm. The total flavonoid content was quantified using a calibration curve based on catechin concentrations ranging from 50 to 500

mg/mL ($r^2 = 0.999$). The results were expressed as milligrams of catechin equivalent (CAT) per gram of dry weight.

Determination of Total Proanthocyanidin Content

Total proanthocyanidin was assayed by the method of White *et al.*, (2010). A mixture containing 3 mL of vanillin-methanol (4% v/v) and 1.5 mL of hydrochloric acid was added to 0.5 mL from 1 mg/mL of lyophilized *Senna alata* extract, vortexed properly. The resultant mixture was left for 15 minutes at RT followed by absorbance measurements at 500 nm. Total proanthocyanidin content expressed as catechin equivalent (mg/g).

Determination of Saponins Contents

The saponin content was analyzed using the spectrophotometric method described by Brunner (1984). To begin, 1 mL of the sample was placed in a 250 mL beaker, and 100 mL of isobutyl alcohol was added. The mixture was then subjected to continuous shaking for 5 hours using a UDY shaker to ensure thorough mixing. The mixture was filtered through Whatman No. 1 filter paper into a 100 mL beaker. To the filtrate, 20 mL of a 40% saturated magnesium carbonate ($MgCO_3$) solution was added. This solution was then filtered again using Whatman No. 1 filter paper to obtain a clear, colorless liquid. After that 1 mL of the clear filtrate was transferred into a 50 mL volumetric flask, and 2 mL of a 5% ferric chloride ($FeCl_3$) solution was added. The volume was adjusted to the 50 mL mark with distilled water, and the mixture was left to stand for 30 minutes to allow a blood-red color to develop. For quantification, standard saponin solutions ranging from 0 to 10 ppm were prepared from a stock saponin solution. These standard solutions were treated in the same manner as the sample, with the addition of 2 mL of 5% $FeCl_3$ solution. The absorbance of both the sample and standard solutions was measured using a Spectronic 21D spectrophotometer at a wavelength of 380 nm. The saponin content was then calculated using the appropriate formula.

$$\text{Saponin } \left(\frac{\text{mg}}{100} \text{ mL} \right) = \frac{\text{Absorbance of sample} \times \text{Average gradient} \times \text{Dilution factor}}{\text{Weight of sample} \times 10,000} \times 100 \quad (1)$$

Determination of Total Terpenoids Content

The tissue samples received tungsten carbide bead treatment before homogenizing them in a 3.5 mL cold bath of 95% methanol. The resulting supernatant derived from centrifugation at 4000 g for 15 minutes was transferred into microcentrifuge tubes. Chloroform was then added to the supernatant, followed by dilution with a Linalool solution prepared in methanol. A series of standard dilutions were created, ranging from 100 mg/200 μ L to 1 mg/200 μ L

(12.965 μ M–1.296 μ M), to establish a standard curve. The sample mixture was then vortexed for uniform mixing and allowed to sit undisturbed for 3 minutes. Then concentrated sulfuric acid (H_2SO_4) was added to each microcentrifuge tube, and the tubes were incubated in the dark for 1.5 to 2 hours. Over time, reddish-brown precipitates formed in each tube. The supernatant was carefully removed without disturbing the precipitates. To fully dissolve the precipitates, 1.5 mL of 95% methanol was added, and the mixture was vortexed thoroughly. The prepared samples were transferred into colorimetric cuvettes, with 95% methanol serving as the blank. The absorbance of each sample was measured at 538 nm. A standard curve was generated using the blank-corrected absorbance of Linalool standards, and the total terpenoid content of the plant samples was determined by calculating their Linalool equivalents based on the regression equation of the standard curve (Ghorai *et al.*, 2012).

Determination of Total Steroid Content

According to Okeke *et al.* (2017), the spectrophotometric method allowed the determination of total steroid content in plant extracts. This method was employed in this analysis with some modifications. 1 mL of the plant extract solution with 10 mL chloroform solution was mixed thoroughly in a test tube and then allowed to stand for 30 minutes to extract all steroids. The chloroform phase received a careful addition of 3 mL concentrated sulfuric acid (H_2SO_4), which lay underneath the solution. The solution was kept without disturbance for 10 minutes; a reddish-brown color was developed at the interface, which confirmed the presence of steroids. The absorbance of the mixture was measured using the spectrophotometer at a wavelength of 420 nm. A calibration curve was prepared using a standard steroid solution, and the total steroid content of the sample was determined by extrapolation from the standard curve. The results were expressed as milligrams of steroid equivalent per gram of dry weight of the extract.

Green Synthesis of Silver Nanoparticle

100 mL of each aqueous extract was added to 900 mL of a 1 mM silver nitrate salt solution ($AgNO_3$). The mixtures in a conical flask were stirred constantly (at 10 rpm) for about 8 hours at room temperature, and the reaction vessel was covered with aluminum foil to avoid $AgNO_3$ auto-reduction due to photosensitivity. The bio-reduction of Ag^+ to Ag^0 resulted in a physical color change of the mixture from a milky yellowish to a darkish-brown after 6 hours of swirling at 15 rpm. A centrifugation process with a speed of 15,000 rpm operated using a centrifuge machine (Model 0508-I) was performed on the blend for ten minutes. The supernatant was discarded before re-dispersing the

formed pellets in distilled water and repeating washing procedures three times to remove all bioactive plant compounds in the mixture. The drying procedure for pellets was conducted under 37°C conditions before they were kept as future research material.

Characterization of Biosynthesized silver nanoparticle

In this study, *Senna alata* silver nanoparticles (SA-AgNPs) were characterized by various physical and chemical techniques to confirm the optical properties, structure, composition, and surface morphology. First, the surface morphology and elemental composition of AgNPs were confirmed by SEM (Merline compact, Zeiss, Germany) coupled with EDS (Rajivgandhi *et al.*, 2022). The shape and particle size distribution of SA-AgNPs were noted with the help of HR-TEM (FEI, Talos F200X G2) and analyzed using Nano Measurer 1.2 software (Yuan *et al.*, 2017a).

XRD crystalline pattern of SA-AgNPs were recorded on a Panalytical Empirian diffractometer (Ultima 4, Japan) with a step size of 0.02° and scan speed of 5°/min in the scan range from 30° to 80° of 2. Using the width of the peak with most pronounced Bragg's reflection as a reference, Debye-equation Scherrer's was used to determine the average crystalline size of the AgNPs (Sharma *et al.*, 2018).

The thermo-stability of the dried SA-AgNPs samples was determined by the use of TGA instruments. Samples were put in 100 µL ceramic pans and equilibrated to 28 °C in the TGA and then heated at a rate of 40-600 °C per minute. During the measurement of the sample, air was introduced to the samples at a rate of 50 mL/min in order to keep the environment around the sample under oxidation (Adebayo *et al.*, 2020). The residue was used to estimate the silver content in the SA-AgNPs.

In Vitro Antioxidant Potential

DPPH Assay

The radical-scavenging and antioxidant activities of the SA-AgNPs, and the lyophilized aqueous extracts were estimated alongside the free radical DPPH, and commercial antioxidants (vitamin C). All the samples were

incubated with a DMSO solution of DPPH for about 30 minutes at room temperature in the dark. A vortex machine was employed to give a thorough vibration of the mixture, and the absorbance was read at 517 nm. The capacity of the crude extracts to hunt for DPPH free radical was calculated using the equation as follows:

$$\text{Inhibition (\%)} = \frac{(A_{\text{Control}} - A_{\text{Sample}})}{A_{\text{Control}}} \times 100 \quad (2)$$

Where, A_{Control} = is the absorbance of DPPH + DMSO and A_{Sample} is the absorbance of DPPH + extracts (aqueous or AgNPs) or the commercial antioxidant (Larayetan *et al.*, 2017). The dose-response curve was plotted, and the IC₅₀ values for the commercial antioxidants and *Senna alata* extracts were determined (Larayetan *et al.*, 2017).

ABTS Assay

The ABTS potencies of both SA-AgNPs and *Senna alata* extracts were determined using a modified Nantitanon *et al.* (2007) approach. The operational solution was obtained by oxidizing ABTS stock solution (7 mM) with 2.4 mM of potassium per sulfate in equal parts, and the mixture was allowed to react for 12 h at room temperature. After 7 min., a UV-spectrophotometer was used to take absorbance reading at 734 nm (0.706 ± 0.001) from a fraction of resulting solution (1 mL). Briefly, different concentrations (0.025 to 0.4 mg/mL) of each extract were added to a methanolic solution of ABTS for 7 minutes under room temperature and in the dark. The absorbance was then recorded spectrophotometrically at 760 nm, and ABTS % inhibition by Vitamin C, SA-extracts (AgNPs and aqueous extracts) and commercial antioxidant, was calculated with the equation described in the DPPH experiment above.

Statistical Analysis

Data was analysed using Microsoft Excel and reported as the mean ± standard deviation of triplicate determinations. In addition to this, nonlinear regression using Prism 5 for Windows, Version 5.02 (Graph Pad Software, Inc) program, was used to resolve IC₅₀ from the dose-response curve (Larayetan *et al.*, 2019).

RESULTS AND DISCUSSION

Phytochemical screening of aqueous extract of *Senna alata*

Table 1: Qualitative Phytochemical Screening of *Senna alata* Lyophilized Extract

S/N	Phytochemical Constituents	Specific Test	Result
1	Alkaloid	Hager's test	-
2	Flavonoid	Sodium Hydroxide test	+
3	Terpenoid	Liebermann-Burchard Test	+
4	Steroids	Salkowski test	+
5	Saponin	Foam test	+
6	Phenols	Ferric chloride test	+
7	Tannin	Braymer's test	+

(+)= Present, (-) = absent.

Table 2: Quantitative Phytochemical Screening of the Leaf Extracts of *S. alata*

Extracts	Phenol mg/100g	Flavonoid mg/100g	Tannin mg/100g	Phytate mg/100g	Saponin mg/100g	Steroid mg/100g	Terpenoid mg/100g	Proanthocyanidin mg/100g
S.Aaq	941.32 ±10.56	638.88 ± 4.45	665.45 ± 10.29	181.22 ± 5.07	16.62 ± 0.73	188.26 ± 2.13	212.96 ± 1.49	145.05 ± 74.45

Key: S.A_{aq} = Aqueous extract of *S. alata*

Phytochemical screening of the lyophilized aqueous extract of *S. alata* has revealed flavonoids, phenols, tannins, terpenoids, steroids, saponins, and proanthocyanidins. Phytochemical qualitative screening of alkaloid was absent in the plant; however, flavonoids, terpenoids, steroids, saponins, phenolic compounds, and tannins are present as revealed in Table 1. Further, quantitative phytochemical analysis as depicted in Table 2 shows a notable amount of these bioactive compounds in *S. alata* aqueous extract. These bioactive compounds stored in plants could be used to make an alternative medicine for treating bacterial infections in human beings due to their biological and antibacterial activities (Bittner-Fialová *et al.*, 2021). Total Tannin, Phenol, Flavonoid, Phytate, Saponin, Steroid, Terpenoid, and Proanthocyanidin Content were determined to be 665.45 ± 10.29 , 941.32 ± 10.56 , 638.88 ± 4.45 , 181.22 ± 5.07 , 16.62 ± 0.73 , 188.26 ± 2.13 , 212.96 ± 1.49 , and 145.05 ± 74.45 mg/100g respectively in the aqueous extract of *S. alata* (table 2). Flavonoids are secondary metabolites of a class of naturally occurring polyphenols. They are widespread in plants. Flavonoids contribute to the production of pigment, which attracts pollinators. Being phytochemicals, flavonoids cannot be synthesized by animals or human beings (Guan *et al.*, 2021). These compounds not only contribute to the main organoleptic characteristics of food, such as flavor and color, but also simultaneously inhibit lipid peroxidation as well as enzyme inactivation and vitamin degradation in food products (Gantner, & Kostyra, 2023). Apart from their role in plant physiology and their value in food preservation, flavonoids have strong pharmacological activity, including reported anti-inflammatory activity, anti-allergic activity, and anti-neoplastic activity (Oršolić, 2022). Of all subclasses of flavonoids, flavonols are distributed most in food sources. Phytates are naturally occurring plant compounds that bind minerals like calcium, iron, and zinc, reducing their bioavailability. They have been linked to several health-promoting functions, including anti-cancer and cholesterol-lowering effects; they have antioxidant properties (Ibrahim *et al.*, 2021). The amount of phytate in

the aqueous extract of *S. alata* gives an idea of the potential nutritional and anti-nutritional effects when the extracts of *S.alata* are consumed because high level of phytate might impact the mineral absorption when it is taken inside the body. Saponins are bioactive compounds, and their pharmacological activities have been well demonstrated in antibacterial, antifungal, anti-inflammatory, and anti-diabetic effects apart from their foaming properties. The compound is also used as an expectorant and in the treatment of respiratory disorders (Rai *et al.*, 2021). The aqueous extract of *S. alata* contained a moderate amount of saponins and might be accountable for its medicinal uses. Steroids are important plant metabolites with medicinal potential as precursors for steroid hormones; they have also been reported to exert anti-inflammatory, analgesic, and immunomodulatory effects (Vazifeh *et al.*, 2022). *S. alata* may have potential applications in the pharmaceutical industry, especially in the production of medications based on steroids. Terpenoids, which have been shown to have antimicrobial, antiviral, anti-inflammatory, and anti-cholesterol properties, are among the most prevalent families of secondary metabolites found in plants (Kumar *et al.*, 2022). They have been under keen investigation in both traditional and modern medicine. Proanthocyanidins are polyphenolic compounds that have been demonstrated to possess potent antioxidant qualities and support cardiovascular health by lowering oxidative stress. They are also believed to have anti-cancer properties (Sabbatino *et al.*, 2021).

The phytochemical screening of the aqueous extract of *S. alata* revealed prominent bioactive compounds, including phenols, flavonoids, tannins, saponins, steroids, terpenoids, and proanthocyanidins. Most of the secondary metabolites, including the above-mentioned phytoconstituents, showed antioxidant, antimicrobial, and anti-inflammatory activities, due to the medicinal values attributed to *S. alata*. High amounts of phenolic compound and terpenoid give credence to the fact that this plant may become an excellent natural source for pharmaceutical and nutraceutical purposes.

Characterization of biosynthesized AgNPs
Thermo-gravimetric analysis and Differential Thermal (TGA/DTA) Analysis

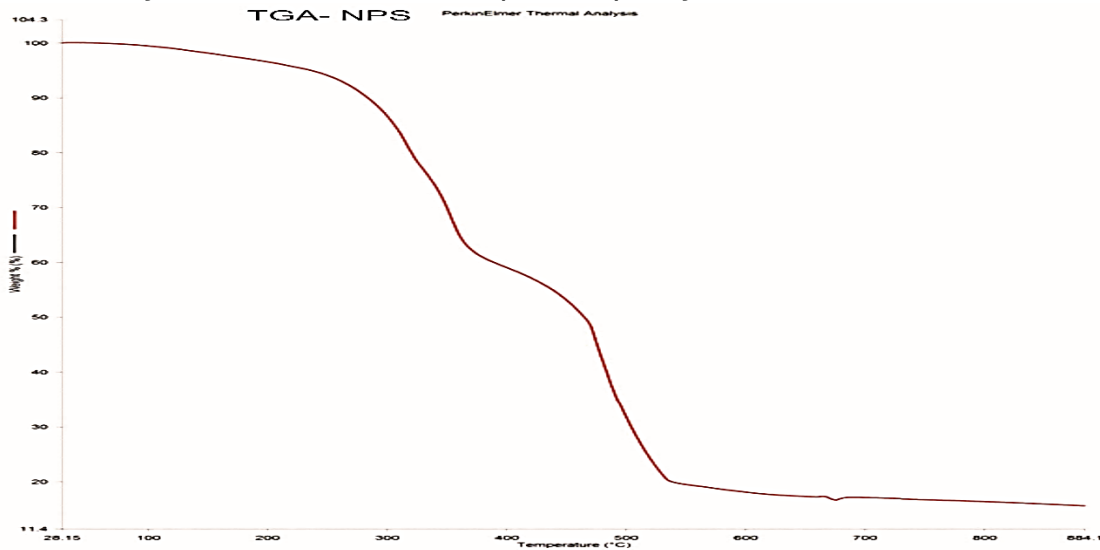


Figure 1: TGA Graph for AgNPs of *S. alata*

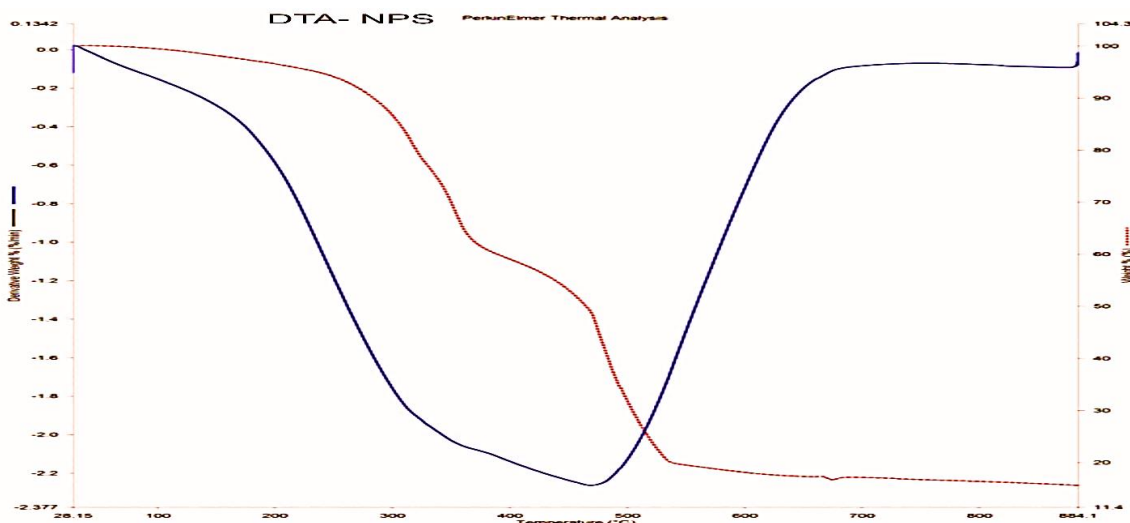


Figure 2: DTA Graph for AgNPs of *S. alata*

Figure 1 is a TGA-NPS graph showing the thermal breakdown behavior of AgNPs as a function of temperature. The figure shows about 4-5% weight loss up to 100°C, which may be associated with the evaporation of the remaining moisture or the adsorbed water molecules on the surface of nanoparticles. The AgNPs then show excellent thermal stability in that a relatively flat and even an area of stability is obtained between 28.15°C and 200°C, which shows that no major decomposition or phase change occurs during this temperature. Above 200°C, the weight percentage curve drops considerably, most likely due to thermal decomposition of organic capping agents or the stabilizers, which have been deposited on AgNP surfaces. Adebayo-Tayo *et al.* (2020) obtained a continuous mass loss with two quasi-sharp

changes at 268.68°C and 485°C followed by a nearly constant plateau. Annealing temperatures higher than 400°C seem to guarantee the stability of the SA-AgNPs. The complementary DTA-NPS elucidates the thermal transitions and phase changes that AgNPs undergo. It brings forth two important endothermic peaks: one at about 100°C, corresponding with the evaporation of adsorbed water, and a broader second peak centered at 350°C, which is attributed to the thermal decomposition of organic capping agents. This stability of AgNPs after heat treatment up to the investigated temperature is proved by the absence of other notable peaks in the DTA graph (Shirinova *et al.*, 2024). The synthesized AgNPs using the *Senna alata* extract are found to be thermally stable up to approximately 400°C from the combined interpretation of

data obtained from TGA-NPS and DTA-NPS studies; however, the organic components are found to start degrading at a higher temperature. This thus makes it very relevant information for the realization of the thermal

behavior and probable uses that the said Nanoparticles may have in aspects such as catalysis, electronics, and biomedicine, in which issues associated with thermal stability are particularly basic (Souza *et al.*, 2022).

Transmission Electron Microscopy (TEM) Analysis

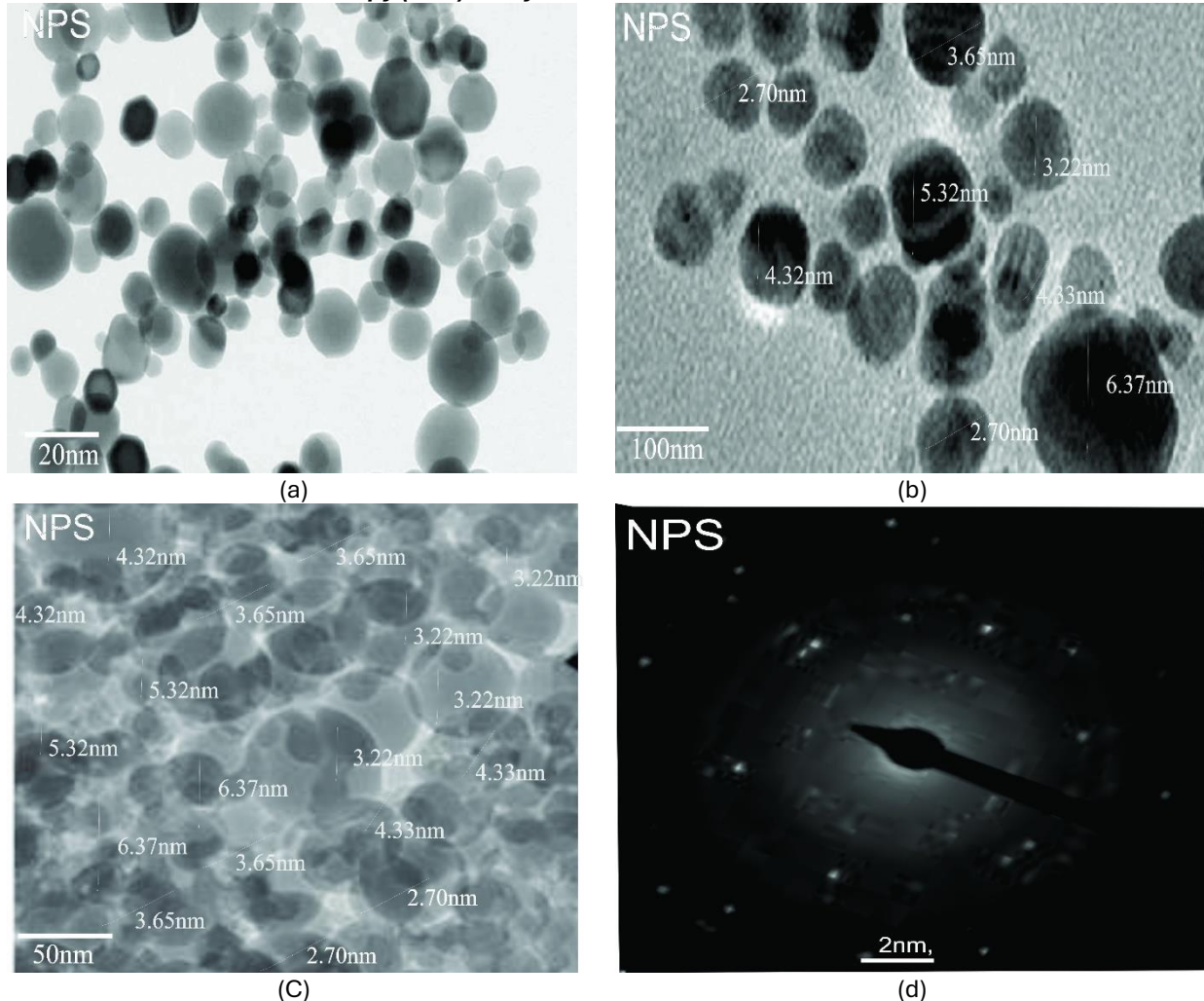


Figure 3A, B, & C: TEM Micrograph images of AgNPs of *S. alata* (D) SAED Micrograph images of AgNPs of *S. alata*

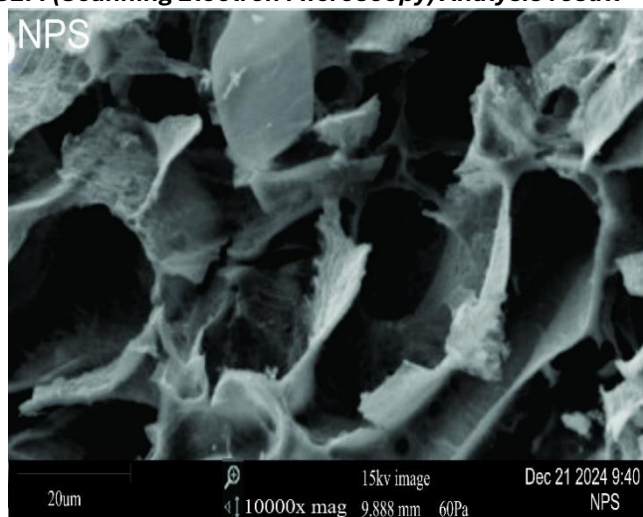
Figure 3A, B, C shows the TEM analysis of the synthesized silver nanoparticles (AgNPs) across different size distribution; it has been found that the AgNPs have a relatively wide range in the diameter sizes, varying from about 2.70 nm to about 6.37 nm. However, the size distribution is relatively homogenous with several prominent fractions at 4.32 nm, 4.33 nm, 3.22 nm, and 3.65 nm. Fouda *et al.* (2020) found that Streptomyces-mediated produced AgNPs were spherical in shape, uniformly distributed without aggregation, and measured between 4.09 and 12.88 nm in size. The generated AgNPs in this work appear to be mainly spherical in shape, with a consistent and unique nanoparticle shape throughout the sample. Veeraraghavan *et al.* (2021) reported that high-resolution TEM images of Sb-AgNP were primarily

spherical in shape and in the size range of 20 to 40 nm. This proves that the synthesized AgNP falls under the nanoscale range of 1-100 nm. With some scattering in the size distribution, the AgNPs still hold high overall uniformity, showing clear dominance of specific size ranges (Lalegani, & Ebrahimi, 2020). This would mean that there is control over the synthesis process and reproducibility, hence yielding a fairly homogeneous population of nanoparticles. Naganthran *et al.* (2022) state that detailed TEM analysis gives quantitative data relating to the physical properties of the synthesized AgNPs, which are very essential in understanding their potential behavior and applications. In any case, in order to evaluate the effectiveness of the synthesis process and to ensure that the nanoparticle attributes are appropriate for the

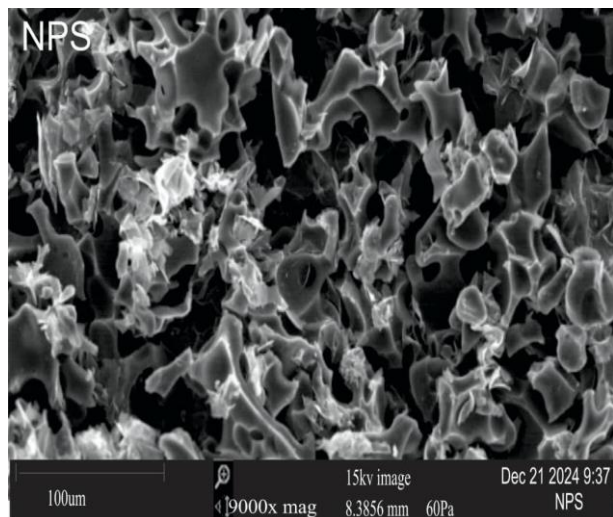
intended uses in a given use case, characterization of the size, shape, and distribution of a nanoparticle system is very fundamental (Khan *et al.*, 2022). As demonstrated by Dubey *et al.* (2023), such nanoscale characterization is very critical to optimize synthesis and unleash the full potential of AgNPs in a variety of applications. The SAED pattern in figure 3D shows the crystalline structure and phase composition of the formed AgNPs. The formation of crystalline AgNPs is confirmed by the clear diffraction spots in the picture. The diffraction spots reflect the face-centered cubic (FCC) crystal structure of metallic silver. The FCC silver crystal lattice can then be identified by the respective diffraction spots corresponding to the (111), (200), (220), and (311) planes (Ali *et al.*, 2023). The presence of a high degree of structural order and high crystalline structure of the AgNPs is evidenced by the distinct and crisp diffraction spots. This is a very desirable

characteristic, as it proves the successful reduction of silver ions and the formation of highly stable and mono-disperse nanoparticles (Jain *et al.*, 2021). The spacing between the diffraction spots is therefore used in determining the interplanar spacing, d-spacing, of the AgNPs crystal lattice. This information, together with the position of the diffraction spots, could then be used to determine the lattice parameters and hence the overall crystallographic structure of the synthesized AgNPs (Ali *et al.*, 2023). It can thus be related that the intensity and sharpness of the diffraction spots are indicative of the size and size distribution of the AgNPs: sharper and more intense spots usually correspond to larger nanoparticles with a narrower size distribution, while wider and less-intense spots suggest smaller nanoparticles with a broader size distribution.

SEM (Scanning Electron Microscopy) Analysis result



(a)



(b)

Figure 4A, & B: SEM images of AgNPs of *S. alata*

Figure 4A and B are the Scanning electron microscope images of synthesized silver nanoparticles using *Senna alata* extract; SEM provides the morphological characteristic and structural features. It gives an overall idea regarding the size, distribution, and surface morphology of the AgNPs. The synthesized nanoparticles are found to have an aggregated, highly irregular, and porous structure; this happens to be a typical characteristic of AgNPs synthesized in the presence of plant-based reducing agents. The particles showed a wide distribution in size, ranging from about 100 nm to more than 9 μm in diameter. This shows that the smaller nanoparticles and the larger agglomerates or aggregates

are formed. The irregular and porous nature of the AgNPs would then suggest that capping agents or stabilizers are attached to the *Senna alata* extract, which desirably reduces agglomeration and maintains the disparity of the nanoparticles (Adebayo-Tayo *et al.*, 2020). The SEM examination gives valuable information on the overall size, morphology, and state of agglomeration of the AgNPs synthesized from the extract of *Senna alata* (Adebayo-Tayo *et al.*, 2020). Such knowledge may help assess the possible applications and performance of nanoparticles besides guiding further process optimization toward a more uniform and controlled nanoparticle characteristic.

EDS (Energy-Dispersive X-ray Spectroscopy) Analysis

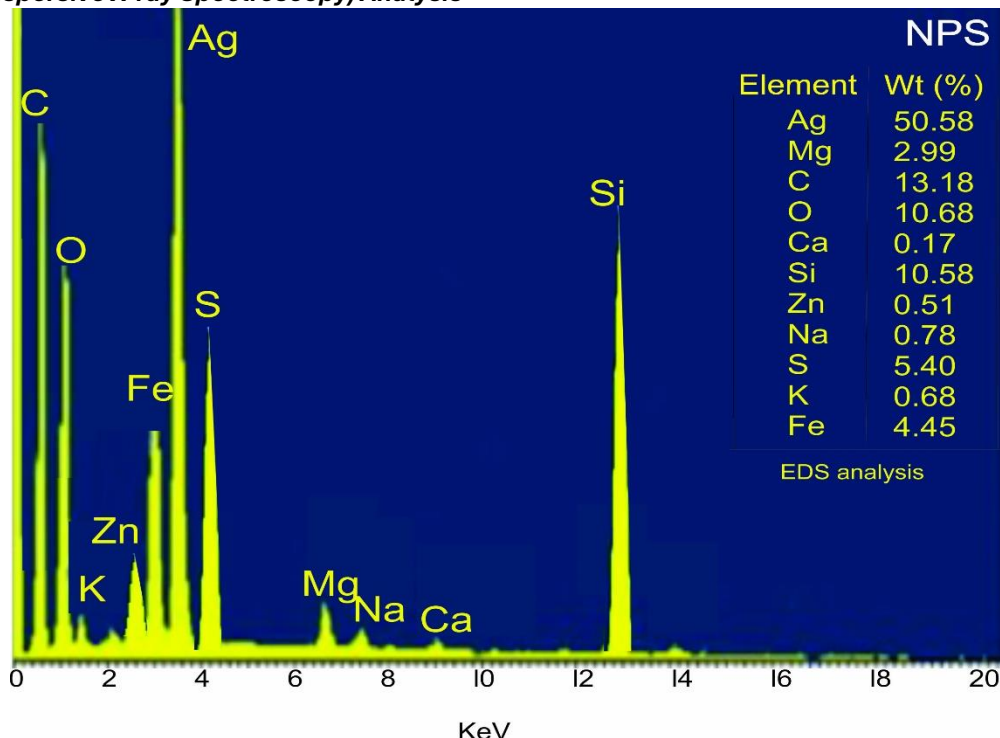


Figure 5: The EDS (Energy-Dispersive X-ray Spectroscopy) of AgNPs

Figure 5 is the EDS (Energy-Dispersive X-ray Spectroscopy) spectrum, EDS gives the elemental composition details of the sample of AgNPs under analysis. Silver is represented by the highest peak in the spectrum at 3.7 keV and represents a huge fraction of the sample (50.58%). It would therefore seem that this material is composed primarily of silver. Sivasubramanian *et al.* (2023) write, "It is evident from the elemental profile of synthesized AgNP from *senna alata*, which shows the highest X-ray energy peak at 3 keV corresponding to silver. The 13.18% carbon may indicate other carbon-based pollutants or organic residues. It may contain oxides or other oxygen-containing compounds because oxygen makes up 10.68 weight percent of it. The observed silicon content of 10.58 weight percent most likely explained the presence of silicates or other compounds containing silicon. Among the minor

elements found, sulfur is present at 5.40%. The 4.45% iron level suggests that there may be iron-containing phases present, most likely oxides or alloys. Magnesium is present at 2.99%, most likely as compounds that include magnesium. The following other minor elements are present in smaller levels and each contribute less than 1%: potassium (K), sodium (Na), zinc (Zn), and calcium (Ca). All the elements within the spectrum have their peaks standing out uniquely, with Ag, Si, and C having the highest intensity peaks. Given a high concentration of silver, the sample is most likely to be metallic silver or silver-based compounds. The presence of carbon, oxygen, iron, magnesium, calcium, zinc, sodium, and sulfur was detected in the plant extract; hence, phytochemicals acted as a capping agent during the production of AgNPs (Yadav *et al.*, 2024).

Antioxidant Analysis

Table 3: Corresponding inhibition percentages of the *Senne alata* Nanoparticles (NPS) and Extracts (EX) at different concentrations using DPPH and ABTS assays.

Concentration (mg/mL)	DPPH Inhibition (%)		ABTS Inhibition (%)	
	NPS	EX	NPS	EX
5	44.73	39.67	47.47	51.10
10	61.80	72.70	61.20	66.20
20	84.98	75.38	71.20	76.65

Table 4: IC₅₀ profile of NPS and EX of *senna alata* leaves.

S/N	Activity	NPS IC ₅₀ mg/mL)	EX IC ₅₀ mg/mL)	Vitamin C mg/mL)	IC ₅₀	Trtlox mM/mL)	IC ₅₀
1	DPPH	0.129	0.134	0.00015	-	-	-
2	ABTS	0.943	0.954	-	-	1.187	-

Antioxidant activity of *Senna alata* NPS and EX was evaluated by two complementary antioxidant assays; DPPH and ABTS (Table 3). Application of the dual-method approach is in agreement with the best practices in antioxidant research, as forwarded by Ravi *et al.* (2024), where it is recommended that multiple methods should be used for the assessment of antioxidant activity. The DPPH assay, which measures the ability to donate electrons or hydrogen atoms, showed concentration-dependent increases in the percentages of inhibition for NPS and EX (Gulcin *et al.*, 2023). At 5 mg/mL, NPS (44.73%) was more inhibited than the EX (39.67%). Now, it's better performance became more apparent with NPS at 84.98% compared to 75.38% for EX at 20 mg/mL. This increased activity at the higher concentrations is a clear indication of more effective radical scavenging by the nanoparticle formulation. The IC₅₀ values (NPS: 0.129 mg/mL; EX: 0.134 mg/mL) affirm this observation.

The ABTS assay provided complementary data and supported the idea that antioxidant evaluation should be done with several models of radicals (Sheng *et al.*, 2021). At the lower concentrations, that is, at 5 mg/mL, the extract (51.10%) performed slightly better than NPS (47.47%). This trend continued at 20 mg/mL, where the extract showed greater inhibition (76.65%) than NPS (71.20%). The formulated drugs scavenge ABTS radicals with the same potency, judged by the IC₅₀ values in close proximity. NPS shows 0.943 mg/mL and EX 0.954 mg/mL. Trolox and vitamin C showed average antioxidant activity in the manufactured drugs, with IC₅₀ values of 1.187 mM/mL for ABTS and 0.00015 mg/mL for DPPH, respectively. According to Kang *et al.* (2023) and Sheikh *et al.* (2024), the formulation's inconsistent effectiveness across assay systems suggests that the antioxidant mechanisms of action of plant components differ from those previously reported by other researchers.

This increased activity of DPPH scavenging by NPS could be related to the incorporation of flavonoids and phenolic compounds that have been well-documented to possess strong free radical-scavenging potential (Shi *et al.*, 2022; Muflihah *et al.*, 2021). This possibly relates to the increased surface area and better accessibility to the active areas, much the same as previously stated in nanoparticle formulations (Larayetan *et al.*, 2019). These results could be of value in disorders associated with oxidative stress; NPS is especially promising in DPPH-mediated oxidative systems, while EX performs well in ABTS-mediated systems.

CONCLUSION

This study on *Senna alata* demonstrated high amounts of helpful substances, particularly flavonoids and phenols; hence, it may have high health benefits. Green synthesis of silver nanoparticles was confirmed by various characterization techniques, with TEM, SEM, SAED, EDS, TGA and DTA analysis showing homogenous spherical particles in the range of 2.70-6.37 nm, crystalline structure, phase composition of the formed AgNPs and thermal stability up to 400°C. Antioxidant assay proved that both nanoparticles and the crude extract possessed appreciable free radical scavenging activity, yet the nanoparticles had a better activity with a DPPH inhibition percentage of 84.98%, whereas the extract was 75.38%. All the findings prove that silver nanoparticles mediated through *S. alata* are an excellent selection in biomedical applications owing to their required antioxidant property.

REFERENCES

- Adebayo-Tayo, B. C., Borode, S. O., Olaniyi, O. A. (2020). "Phytosynthesis of zinc oxide nanoparticles using methanol extract of *Senna alata* leaf: Characterization, optimization, antimicrobial properties, and its application in cold cream formulation", *Polimers in Medicine*, 50(1), pp. 5–19. <https://doi.org/10.17219/pim/122901>
- Ahmad, A., Haneef, M., Ahmad, N., Kamal, A., Jaswani, S., & Khan, F. (2024). Biological synthesis of silver nanoparticles and their medical applications. *World Academy of Sciences Journal*, 6(3), 22.
- Ali, M. H., Azad, M. A. K., Khan, K. A., Rahman, M. O., Chakma, U., & Kumer, A. (2023). Analysis of crystallographic structures and properties of silver nanoparticles synthesized using PKL extract and nanoscale characterization techniques. *ACS omega*, 8(31), 28133-28142.
- Bittner Fialová, S., Rendeková, K., Mučaji, P., Nagy, M., & Slobodníková, L. (2021). Antibacterial activity of medicinal plants and their constituents in the context of skin and wound infections, considering European legislation and folk medicine—a review. *International Journal of Molecular Sciences*, 22(19), 10746.
- Boateng, J. (Ed.). (2020). *Therapeutic dressings and wound healing applications*. John Wiley & Sons.

Brunner, G. (1984). Mass transfer from solid material in gas extraction. *Berichte der Bunsengesellschaft für physikalische Chemie*, 88(9), 887-891.

Chang, C. C., Yang, M. H., Wen, H. M., & Chern, J. C. (2002). Estimation of total flavonoid content in propolis by two complementary colorimetric methods. *Journal of food and drug analysis*, 10(3).

Chua, L. Y. W., Chua, B. L., Figiel, A., Chong, C. H., Wojdyto, A., Szumny, A., & Lech, K. (2019). Characterisation of the convective hot-air drying and vacuum microwave drying of *Cassia alata*: Antioxidant activity, essential oil volatile composition and quality studies. *Molecules*, 24(8), 1625.

Dubey, R. K., Shukla, S., & Hussain, Z. (2023). Green Synthesis of Silver Nanoparticles; A Sustainable Approach with Diverse Applications. *Chinese Journal of Applied Physiology*, e20230007.

Fatmawati, S., Yuliana, P. A., & Abu Bakar, M. F. (2020). Chemical constituents, usage and pharmacological activity of *Cassia alata*. *Heliyon*; 6 (7): e04396.

Fouda, A., Hassan, S.E.D., Abdo, A.M., El-Gamal, M.S., (2020). Antimicrobial, antioxidant and larvicidal activities of spherical silver nanoparticles synthesized by endophytic *Streptomyces* spp. *Biological Trace Element Research*, 195(2), pp.707-724.

Gantner, M., & Kostyra, E. (2023). Special Issue on the Latest Research on Flavor Components and Sensory Properties of Food during Processing and Storage. *Foods*, 12(20), 3761.

Ghorai, N., Chakraborty, S., Gucchait, S., Saha, S. K., and Biswas, S. (2012). Estimation of total Terpenoids concentration in plant tissues using a monoterpene, Linalool as standard reagent. *Journal of pharmacognosy and phytochemistry*

Guan, R., Van Le, Q., Yang, H., Zhang, D., Gu, H., Yang, Y., ...& Peng, W. (2021). A review of dietary phytochemicals and their relation to oxidative stress and human diseases. *Chemosphere*, 271, 129499.

Gulcin, İ., & Alwasel, S. H. (2023). DPPH radical scavenging assay. *Processes*, 11(8), 2248.

Gunjal, A., Patwardhan, R., Jedhe, A., & Choudhary, V. (2022). Plasmid-Curing, Antimicrobial, Antioxidant Properties and Phytochemical Analysis of Medicinal Plants

from North East India.(2021). *Int. J. Life Sci. Pharma Res*, 11(1), P100-109.

Gupta, V. K., Simlai, A., Tiwari, M., Bhattacharya, K., & Roy, A. (2014). Phytochemical contents, antimicrobial and antioxidative activities of *Solanumsisymbriifolium*. *Journal of Applied Pharmaceutical Science*, 4(3), 075-080.

Herrero-Calvillo R, Landeros-Páramo L, Santos-Ramos I, Rosas G. (2022). AgNPs/AgCl cube-shaped particles synthesized by a green method and their catalytic application. *Journal of Cluster Science*.8:1-9.

Ibrahim, M. R., Hamouda, R. A., Tayel, A. A., & Al-Saman, M. A. (2021). Anti-cholesterol and antioxidant activities of independent and combined microalgae aqueous extracts in vitro. *Waste and Biomass Valorization*, 12, 4845-4857.

Jain, A. S., Pawar, P. S., Sarkar, A., Junnuthula, V., & Dyawanapelly, S. (2021). Bionanofactories for green synthesis of silver nanoparticles: Toward antimicrobial applications. *International Journal of Molecular Sciences*, 22(21), 11993.

Kang, S., Kim, Y., Lee, Y., & Kwon, O. (2023). Diverse and Synergistic Actions of Phytochemicals in a Plant-Based Multivitamin/Mineral Supplement against Oxidative Stress and Inflammation in Healthy Individuals: A Systems Biology Approach Based on a Randomized Clinical Trial. *Antioxidants*, 13(1), 36.

Kędziora, A., Wieczorek, R., Speruda, M., Matolínová, I., Goszczyński, T. M., Litwin, I., ...& Bugla-Płoskońska, G. (2021). Comparison of antibacterial mode of action of silver ions and silver nanoformulations with different physico-chemical properties: Experimental and computational studies. *Frontiers in Microbiology*, 12, 659614.

Khan, Y., Sadia, H., Ali Shah, S. Z., Khan, M. N., Shah, A. A., Ullah, N., ... & Khan, M. I. (2022). Classification, synthetic, and characterization approaches to nanoparticles, and their applications in various fields of nanotechnology: A review. *Catalysts*, 12(11), 1386.

Kumar, S., Saini, R., Suthar, P., Kumar, V., & Sharma, R. (2022). Plant secondary metabolites: Their food and therapeutic importance. In *Plant secondary metabolites: Physico-chemical properties and therapeutic applications* (pp. 371-413). Singapore: Springer Nature Singapore.

Lalegani, Z., & Ebrahimi, S. S. (2020). Optimization of synthesis for shape and size controlled silver

- nanoparticles using response surface methodology. *Colloids and Surfaces A: Physicochemical and Engineering Aspects*, 595, 124647.
- Larayetan, R. A., Okoh, O. O., Sadimenko, A., & Okoh, A. I. (2017). Terpene constituents of the aerial parts, phenolic content, antibacterial potential, free radical scavenging and antioxidant activity of *Callistemon citrinus* (Curtis) Skeels (Myrtaceae) from Eastern Cape Province of South Africa. *BMC complementary and alternative medicine*, 17, 1-9.
- Larayetan, R., Ojemaye, M. O., Okoh, O. O., & Okoh, A. I. (2019). Silver nanoparticles mediated by *Callistemon citrinus* extracts and their antimalaria, antitrypanosoma and antibacterial efficacy. *Journal of Molecular Liquids*, 273, 615-625.
- Loganathan, S., Selvam, K., Padmavathi, G., Shivakumar, M. S., Senthil-Nathan, S., Sumathi, A. G., ...& Almutairi, S. M. (2022). Biological synthesis and characterization of *Passiflorasubpeltata* Ortega aqueous leaf extract in silver nanoparticles and their evaluation of antibacterial, antioxidant, anti-cancer and larvicidal activities. *Journal of King Saud University-Science*, 34(3), 101846.
- Muflihah, Y. M., Gollavelli, G., & Ling, Y. C. (2021). Correlation study of antioxidant activity with phenolic and flavonoid compounds in 12 Indonesian indigenous herbs. *Antioxidants*, 10(10), 1530.
- Naganthran, A., Verasoundarapandian, G., Khalid, F. E., Masarudin, M. J., Zulkharnain, A., Nawawi, N. M., ...& Ahmad, S. A. (2022). Synthesis, characterization and biomedical application of silver nanoparticles. *Materials*, 15(2), 427.
- Nantitanon, W., Chowwanapoonpohn, S., & Okonogi, S. (2007). Antioxidant and antimicrobial activities of *Hyptis suaveolens* essential oil. *Scientia Pharmaceutica*, 75(1), 35-54.
- Okeke, E. S., Anosike, C. A., & Nwankwo, J. O. (2017). Spectrophotometric determination of total steroid content in medicinal plant extracts. *Journal of Phytochemical Research*, 5(2), 45-52.
- Oršolić, N. (2022). Allergic inflammation: Effect of propolis and its flavonoids. *Molecules*, 27(19), 6694.
- Osunga, S., Amuka, O., Machocho, A. K., & Getabu, A. (2023). Ethnobotany of some members of the genus *Cassia* (Senna). *Int J Novel Res Life Sci*, 10(5), 1-14.
- Rai, M. K., Deshmukh, S. D., Ingle, A. P., & Gade, A. K. (2012). Silver nanoparticles: the powerful nanoweapon against multidrug-resistant bacteria. *Journal of applied microbiology*, 112(5), 841-852.
- Rai, S., Acharya-Siwakoti, E., Kafle, A., Devkota, H. P., & Bhattarai, A. (2021). Plant-derived saponins: a review of their surfactant properties and applications. *Sci*, 3(4), 44.
- Rajivgandhi, G., Ramachandran, G., Chackaravarthi, G., Chelliah, C. K., Maruthupandy, M., Quero, F., et al. (2022). Preparation of antibacterial Zn and Ni substituted cobalt ferrite nanoparticles for efficient biofilm eradication. *Anal. Biochem.* 653:114787. <https://doi.org/10.1016/j.ab.2022.114787>
- Ravi, G., VenkataDasu, V., & Pakshirajan, K. (2024). A comparative evaluation of batch and fed-batch cultures for enhanced lipid, carotenoid, and β -carotene production by *Rhodotorulamucilaginosa*. *Preparative Biochemistry & Biotechnology*, 1-14.
- Sabbatino, F., Conti, V., Liguori, L., Polcaro, G., Corbi, G., Manzo, V., ...& Pepe, S. (2021). Molecules and mechanisms to overcome oxidative stress inducing cardiovascular disease in cancer patients. *Life*, 11(2), 105.
- Sharma, M., Nayak, P. S., Asthana, S., Mahapatra, D., Arakha, M., and Jha, S. (2018). Biofabrication of silver nanoparticles using bacteria from mangrove swamp. *IET Nanobiotechnol.* 12, 626-632. doi: 10.1049/iet-nbt.2017.0205
- Sheikh, Z. N., Sharma, V., Raina, S., Bakshi, P., Zari, A., Zari, T. A., & Hakeem, K. R. (2024). Phytochemical screening, HPLC fingerprinting and in vitro assessment of therapeutic potentials of different apricot cultivars against diabetes, Alzheimer's disease and cancer. *Heliyon*, 10(19).
- Sheng, Z., Jiang, Y., Liu, J., & Yang, B. (2021). UHPLC-MS/MS analysis on flavonoids composition in *Astragalusmembranaceus* and their antioxidant activity. *Antioxidants*, 10(11), 1852.
- Shi, L., Zhao, W., Yang, Z., Subbiah, V., & Suleria, H. A. R. (2022). Extraction and characterization of phenolic compounds and their potential antioxidant activities. *Environmental Science and Pollution Research*, 29(54), 81112-81129.
- Shirinova, H. A., Surkhayli, A. E., Pashayev, B. G., Mammadov, H. M., Jafarov, M. A., & Gahramanli, L. R. (2024). Preparation, characterization and thermal properties of the PS+ Si based polymer

nanocomposites. *Journal of Thermoplastic Composite Materials*, 08927057241288195.

Singh, H., Desimone, M. F., Pandya, S., Jasani, S., George, N., Adnan, M., & Alderhami, S. A. (2023). Revisiting the green synthesis of nanoparticles: uncovering influences of plant extracts as reducing agents for enhanced synthesis efficiency and its biomedical applications. *International Journal of Nanomedicine*, 4727-4750.

Sivasubramanian, P., Kumar, M., Kirankumar, V. S., Samuel, M. S., Dong, C. D., & Chang, J. H. (2023). Capacitive deionization and electrosorption techniques with different electrodes for wastewater treatment applications. *Desalination*, 559, 116652.

Souza, R. R., Gonçalves, I. M., Rodrigues, R. O., Minas, G., Miranda, J. M., Moreira, A. L., ...& Moita, A. S. (2022). Recent advances on the thermal properties and applications of nanofluids: From nanomedicine to renewable energies. *Applied Thermal Engineering*, 201, 117725.

Vazifeh, S., Kananpour, P., Khalilpour, M., Eaisalou, S. V., & Hamblin, M. R. (2022). Anti-inflammatory and Immunomodulatory Properties of *Lepidium sativum*. *BioMed Research International*, 2022(1), 3645038.

Veeraraghavan, V. P., Periadurai, N. D., Karunakaran, T., Hussain, S., Surapaneni, K. M., & Jiao, X. (2021). Green synthesis of silver nanoparticles from aqueous extract of

Scutellariabarbata and coating on the cotton fabric for antimicrobial applications and wound healing activity in fibroblast cells (L929). *Saudi journal of biological sciences*, 28(7), 3633-3640.

Waterhouse, A. L. (2002). Determination of total phenolics. *Current protocols in food analytical chemistry*, 6(1), 11-1.

White, B. L., Howard, L. R., & Prior, R. L. (2010). Polyphenolic composition and antioxidant capacity of extruded cranberry pomace. *Journal of agricultural and food chemistry*, 58(7), 4037-4042.

Wulandari, I. O., Pebriatin, B. E., Valiana, V., Hadisaputra, S., Ananto, A. D., & Sabarudin, A. (2022). Green synthesis of silver nanoparticles coated by water soluble chitosan and its potency as non-alcoholic hand sanitizer formulation. *Materials*, 15(13), 4641.

Yadav, S., Nadar, T., Lakkakula, J., & Wagh, N. S. (2024). Biogenic Synthesis of Nanomaterials: Bioactive Compounds as Reducing, and Capping Agents. In *Biogenic Nanomaterials for Environmental Sustainability: Principles, Practices, and Opportunities* (pp. 147-188). Cham: Springer International Publishing.

Yuan, G., Chen, Y., Li, F., Zhou, R., Li, Q., Lin, W., et al. (2017a). Isolation of an antibacterial substance from *Mahonia fortunei* and its biological activity against *Xanthomonas oryzae* pv. *oryzicola*. *J Phytopathol*. 65, 289–296. <https://doi.org/10.1111/jph.12561>